Chemical Science

EDGE ARTICLE

View Article Online
View Journal | View Issue

Cite this: *Chem. Sci.*, 2019, **10**, 10779

All publication charges for this article have been paid for by the Royal Society of Chemistry

Received 6th August 2019
Accepted 6th October 2019

DOI: 10.1039/c9sc03915e

rsc.li/chemical-science

First experimental evidence for the elusive tetrahedral cations $[EP_3]^+$ (E = S, Se, Te) in the condensed phase†

Philippe Weis,[a] David Christopher Röhner,[a] Richard Prediger,[a] Burkhard Butschke,[a] Harald Scherer,[a] Stefan Weber[b] and Ingo Krossing *[a]

Condensed phase access to the unprecedented tetrahedral cations $[EP_3]^+$ (E = S, Se, Te) was achieved through the reaction of ECl_3[WCA] with white phosphorus ($[WCA]^- = [Al(OR^F)_4]^-$ and $[F(Al(OR^F)_3)_2]^-$; $-R^F = -C(CF_3)_3$). Previously, $[EP_3]^+$ was only known from gas phase MS investigations. By contrast, the reaction of ECl_3[A] with the known P_3^{3-} synthon Na[Nb(ODipp)$_3$(P_3)] (enabling AsP_3 synthesis), led to formation of P_4. The cations $[EP_3]^+$ were characterized by multinuclear NMR spectroscopy in combination with high-level quantum chemical calculations. Their bonding situation is described with several approaches including *Atoms in Molecules* and *Natural Bond Orbital* analysis. The first series of well-soluble salts ECl_3[WCA] was synthesized and fully characterized as starting materials for the studies on this elusive class of $[EP_3]^+$ cations. Yet, with high $[ECl_3]^+$ fluoride ion affinity values between 775 (S), 803 (Se) and 844 (Te) kJ mol^{-1}, well exceeding typical phosphenium ions, these well-soluble ECl_3[WCA] salts could be relevant in view of the renewed interest in strong (also cationic) Lewis acids.

Introduction

The chemistry of simple tetrahedral main group clusters continues to fascinate researchers worldwide.[1–5] Neutral white phosphorus (P_4) is the archetype of this class and a commodity chemical. Even nitrogen was shown to exist shortly as N_4 in a plasma and has raised significant theoretical interest.[6] However, the heavier homologous yellow arsenic (As_4) is difficult to handle due to its high sensitivity to light. Recent years yielded several new representatives, such as AsP_3 (Scheme 1) and As_2P_2, As_3P and SbP_3.[2,7] In addition, a focus was put on the development of chemical tools to facilitate the handling of As_4 with reagents such as $Ag(As_4)_2[Al(OR^F)_4]$ or As_4 intercalated in porous carbon that acts as a storage form of yellow arsenic and yields concentrated solutions of As_4 that are light stable for several hours.[4,8] These molecules continue to offer interesting follow-up chemistry that is not exhausted yet.[9] For example, the side-on protonation of P_4, $[HP_4]^+$ has only been realized very recently.[10] In addition to these neutral molecules, the syntheses and structures of a multitude of Zintl-type anionic tetrahedra shown in Scheme 1 are known: $[Tt_4]^{4-}$ (Tt = Si, Ge, Sn, Pb) or binary anions such as $[Tt_2Pn_2]^{2-}$ (Pn = P, As, Sb, Bi), $[TrPn_3]^{2-}$ (Tr = Ga, In, Tl) and $[TlSn_3]^{5-}$.[11] These are often accessible by solid-state reactions of the corresponding elements with alkaline metals. Several of these long known tetrahedra were also observed in polar media like liquid ammonia and/or with the presence of cryptands and crown ethers as sequestering reagents.[12] Recent additions detected by NMR spectroscopy include the dissolved Zintl-tetrahedra $[Si_4]^{4-}$, $[Sn_4]^{4-}$ and the protonation product ion $[HSi_4]^{3-}$.[13,14] However, the only reports on any cationic tetrahedra are those on $[SP_3]^+$ and $[SeP_3]^+$ as well as the arsenic homologues that were observed by MS in the gas phase as fragmentation products of Pn_4E_3 (Pn = P, As; E = S, Se); the first observation dating back to 1971.[15] Tellurium analogues have not been described in any phase.[16] If turning to coordination chemistry, also no clear evidence for such cations

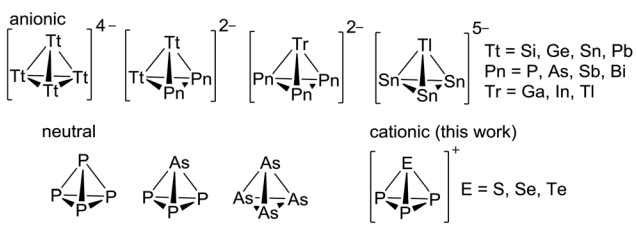

Scheme 1 Exemplary overview of commonly known and structurally characterized tetrahedron shaped molecules in the condensed phase. The cations characterized in this work – albeit without crystal structure – are included for comparison.

[a]*Institut für Anorganische und Analytische Chemie, Freiburger Materialforschungszentrum (FMF), Universität Freiburg, Albertstr. 21, 79104 Freiburg, Germany. E-mail: krossing@uni-freiburg.de*

[b]*Institut für Physikalische Chemie, Universität Freiburg, Albertstr. 21, 79104 Freiburg, Germany*

† Electronic supplementary information (ESI) available. CCDC 1860640, 1898379, 1898380, 1898381 and 1898382. For ESI and crystallographic data in CIF or other electronic format see DOI: 10.1039/c9sc03915e

is published. Only the related complexes $[(triphos)Co(Pn_2E)][BF_4]$ (Pn = P, As; E = S, Se, Te); triphos = 1,1,1-tris(diphenylphosphinomethylethane) are known. Tentatively, these were formulated as coordinated $[P_2E]^+$ and $[As_2E]^+$ cations stemming from the fragmentation of the elusive $[EP_3]^+$ cations.[17] Thus, to the best of our knowledge there is no proven condensed phase evidence for such binary tetrahedral main group cations in any composition.

Despite a large number of binary pnictogen–chalcogen cations of nitrogen, arsenic, antimony and bismuth has been published,[18,19] the first binary phosphorus–chalcogen cation isolated in the condensed phase, $[P_3Se_4]^+$, was only published in 2015 by three independent groups *via* three different routes.[20] Binary phosphorus–sulfur and phosphorus–tellurium cations remain unknown.[21] The $[P_3Se_4]^+$ cation adopts a nortricyclane-like structure similar to the heavier analogues $[As_3S_4]^+$ and $[As_3Se_4]^+$ known since 1981.[19] Attempts to synthesize binary phosphorus–selenium cations by reaction of liquid phosphine PH_3 with $SeCl_3[AlCl_4]$ yielded insoluble polymeric materials[22] tentatively assigned as "$SeP[AlCl_4]_n$".[23] Moreover, most known $[ECl_3]X$ salts (X = suitable anion) are poorly soluble in solvents compatible with white phosphorus. Therefore, any follow-up chemistry of $[ECl_3]X$ salts is scarce and, to our knowledge, in particular no reactions of any trihalochalcogenonium ion with P_4 or any other elemental pnictogen was hitherto published. The synthesis of well soluble $[ECl_3]X$ salts in common solvents is a prerequisite for such investigations and was the starting point for our studies on the tetrahedral $[EP_3]^+$ cations (E = S, Se and Te).

Results and discussion

First attempts towards the synthesis of the $[EP_3]^+$ cations were performed in analogy to the published synthesis[2] of AsP_3 from $Na[Nb(ODipp)_3(P_3)]$ and $AsCl_3$. Thus, $AsCl_3$ was replaced by isoelectronic $ECl_3[WCA]$ (WCA = weakly coordinating anion). Therefore, we briefly describe the synthesis of a series of well soluble $ECl_3[WCA]$ salts before turning to the investigated routes towards the $[EP_3]^+$ cations.

Synthesis of well-soluble $ECl_3[WCA]$ salts as starting materials

The large majority of the many known salts $[EX_3]A$ (E = S, Se, Te, X = F, Cl, Br, I) feature halometallate counterions A like $[AlCl_4]^-$, $[MF_6]^-$ (M = Sb, As) and $[AuCl_4]^-$.[24] They were synthesized from melts or in oxidizing media like $SOCl_2$ or SO_2Cl_2.[24] Typically, they do exhibit poor solubility in common organic solvents. In addition, many of the media employed for synthesis, would be highly reactive towards reductants such as P_4. Therefore, salts $EX_3[WCA]$ (E = S, Se, Te, X = F, Cl, Br, I) soluble in common, non-reactive solvents were needed. Since the WCAs $[Al(OR^F)_4]^-$ and $[F(Al(OR^F)_3)_2]^-$ often lend high solubility to salts of the respective cations, the salts $ECl_3[WCA]$ were prepared by halide abstraction of the chalcogen tetrachlorides with $M[Al(OR^F)_4]$ or $M[F(Al(OR^F)_3)_2]$ (M = Ag, Tl for E = Se; M = Ag for E = Te) in CH_2Cl_2 or liquid SO_2. Eqn (1) is related to the known synthesis of $TeCl_3[Al(OR^F)_4]$ (**2a**).[25]

$$\underset{(M = Ag, Tl;\, E = Se, Te)}{M[WCA] + ECl_4} \xrightarrow[-MCl]{SO_2(liq.)\text{or } CH_2Cl_2} ECl_3[WCA] \quad (1)$$

$$Ag[WCA] + \frac{1}{8}S_8 \xrightarrow[-AgCl]{CH_2Cl_2+\text{exc. } Cl_2} SCl_3[WCA] \quad (2)$$

The compounds $SeCl_3[Al(OR^F)_4]$ (**1a**), $SeCl_3[F(Al(OR^F)_3)_2]$ (**1b**), $SeCl_3[FAl(OR^F)_3]$ (**1c**) and $TeCl_3[F(Al(OR^F)_3)_2]$ (**2b**) are well accessible and soluble in organic media like CH_2Cl_2 and 1,2-$F_2C_6H_4$ (*o*-dfb). By contrast, $[SCl_3]^+$ salts turned out to be very reactive. Due to the instability of SCl_4, it was prepared as an intermediate by the reaction of sulfur with Cl_2 in CH_2Cl_2 and slowly warming the reaction mixture from −196 °C to room temperature. Reaction of this SCl_4 intermediate with $Ag[Al(OR^F)_4]$ according to eqn (2) was accompanied by anion decomposition and yielded predominantly $SCl_3[F(Al(OR^F)_3)_2]$ (**3**). A selective way to **3** in good yields (>90%) simply substitutes $[Al(OR^F)_4]^-$ with the more stable[26–29] anion $[F(Al(OR^F)_3)_2]^-$. Care needs to be taken, to ensure a complete reaction during the synthesis of the $ECl_3[WCA]$ salts. If there is residual $Ag[WCA]$ present in $ECl_3[WCA]$, $Ag(P_4)_2[Al(OR^F)_4]$ or $Ag(P_4)_2[F(Al(OR^F)_3)_2]$ tend to crystallize from the reaction mixtures in subsequent reactions. This could be overcome by using $Tl[WCA]$ as a starting material.[30] Attempts to synthesize $[SeCl_3]^+$ salts from $Li[Al(OR^F)_4]$ and $SeCl_4$ or through metathesis reaction with $SeCl_3[AlCl_4]$ only led to the re-isolation of the starting materials (see ESI Section 3.5†). Since it appeared useful to also test a $[EF_3]^+$ source as starting material, we investigated the preparation of $SF_3[Al(OR^F)_4]$ from $Li[Al(OR^F)_4]$ and SF_4, but all efforts of its synthesis failed (see ESI Section 3.5†). Attempts to synthesize **1b** by reacting $SeCl_4$ with two equivalents of the strong Lewis acid $Me_3Si–F–Al(OR^F)_3$ and trying to skip the synthesis of $Ag[F(Al(OR^F)_3)_2]$, only led to methylation and the isolation of $SeMeCl_2[F(Al(OR^F)_3)_2]$.[31] Yet, to all prepared salts $ECl_3[WCA]$, optimized routes were found and the products were fully characterized (yields, NMR, IR, Raman; crystal structures of **1a**, **1b**, **1c** and **3**). As a side, the crystal structure of $Tl[Al(OR^F)_4]$ was determined and deposited with the CCDC. Due to the well-known properties of the long-known $[ECl_3]^+$ cations, the characterization and discussion of the novel salts $ECl_3[WCA]$ is found in the ESI.†

Syntheses directed towards the ion $[EP_3]^+$

Reaction of 1a with $Na[Nb(ODipp)_3(P_3)]$. In analogy to the published route[2] to AsP_3 from $Na[Nb(ODipp)_3(P_3)]$ and $AsCl_3$, the reaction of **1a** with the P_3^{3-} transfer reagent was tested by weighing equal amounts of the powders into an NMR-tube and condensing a solvent (CD_2Cl_2, 1,2,3,4-tfb (=1,2,3,4-tetrafluorobenzene) or *o*-dfb) onto the sample at −196 °C. The samples were then kept at −40 °C to avoid a reaction of **1a** with the arene. However, the formation of the desired $[SeP_3]^+$ was never observed. Instead, P_4 was cleanly synthesized as indicated by its exclusive signal in the ^{31}P-NMR spectra next to the known signal of the $[Nb(ODipp)_3(P_3)]^-$ anion. Due to the highly chlorinating nature of $[SeCl_3]^+$ compared to the relatively inert $AsCl_3$, the selenonium salt presumably formed PCl_3 by chlorination of

the $[Nb(ODipp)_3(P_3)]^-$ anion. This was followed by an immediate reaction of PCl_3 with the residual $Na[Nb(ODipp)_3(P_3)]$ to form P_4 (ESI, Section 3.3†).

Reactions of ECl_3[WCA] with P_4. Thus, we turned to a different reaction sequence: when reacting $SeCl_3[AlCl_4]$ with P_4 in CH_2Cl_2, a mixture of almost exclusively PCl_3 and $PCl_4[AlCl_4]$ (see ESI Section 3.4.2†) was obtained, next to a red precipitate, supposedly Se_{red}. Yet, the ^{31}P-NMR spectra of this reaction did include a tiny resonance at $\delta^{31}P = -360.8$ hinting towards the formation of $[SeP_3]^+$. Upon changing to the well soluble salts ECl_3[WCA] ($[WCA]^- = [Al(OR^F)_4]^-$, $[F(Al(OR^F)_3)_2]^-$; **1a** to **3**), product ion mixtures containing mainly $[EP_3]^+$ ($[SeP_3]^+$ (**4**), $[TeP_3]^+$ (**5**), $[SP_3]^+$ (**6**)) – easily distinguishable by their characteristic NMR signals (Fig. 1) – and the chlorinated $[P_5Cl_2]^+$ cation were obtained (molar ratio $[EP_3]^+ : [P_5Cl_2]^+ = 0.3$ (E = S), 1.1 (E = Se), 0.3 (E = Te)).

Multiple efforts testing both, the $[Al(OR^F)_4]^-$ and the $[F(Al(OR^F)_3)_2]^-$ anion, to crystallize the obtained product ions **4**, **5** and **6** as pure salts from the complex reaction mixtures were unsuccessful in many solvents. Since the crystal structure of **1c** did show no superstructure and no disorder, as contrasted by the other $[SeCl_3]^+$ salts, **1c** was tested for the synthesis of **4**. This was also futile (see ESI Section 3.4.2†): the $[FAl(OR^F)_3]^-$ anion is not able to withstand the fluorophilic nature of phosphorus cations, and decomposes with formation of several P–F bond containing compounds in the ^{31}P-NMR ($PF_4(OR^F)$, dynamic PF_3 complexes, unknown PF_2X, PFX_2).

Towards optimized reaction conditions. The ratio of $[EP_3]^+$ to $[P_5Cl_2]^+$ in the reaction is highest for $[SeCl_3]^+$ amongst the $[ECl_3]^+$ starting materials. Equal amounts of both cations were obtained in the reaction with $[SCl_3]^+$ and with $[TeCl_3]^+$. Keeping the reaction temperature at −40 °C leads to $[SeP_3]^+$ being around 48% (compared to 28% with the starting conditions) of the total intensity of the cation signals in the ^{31}P spectrum (23% including unremoved PCl_3, see ESI Table S7†) and increases the ratio $[SeP_3]^+ : [P_5Cl_2]^+$ from 1.1 to 1.9 : 1 (Fig. 2).[32] Slow anion decomposition was observed in the ambient temperature ^{19}F-NMR spectra. This can be avoided by keeping the reaction at −40 °C. Screenings of the reaction in different solvents did show no significant improvement for the selectivity of the reaction and led to further side reactions (see ESI Section 3.4.1†). In agreement with this, the calculated Gibbs reaction energies in solvents of different relative dielectric permittivity (CH_2Cl_2, *o*-dfb, SO_2) using the COSMO model revealed no significant solvent dependency (discussion below, Table 2). Experiments using CS_2 to enhance the solubility of P_4 have shown no formation of **4** at all. Raman spectra obtained from reactions on a small scale have only shown fluorescence. Only bulk material obtained from experiments on a larger scale did yield Raman spectra. The vibrational bands can be assigned to the $[Al(OR^F)_4]^-$ anion and tentatively to the

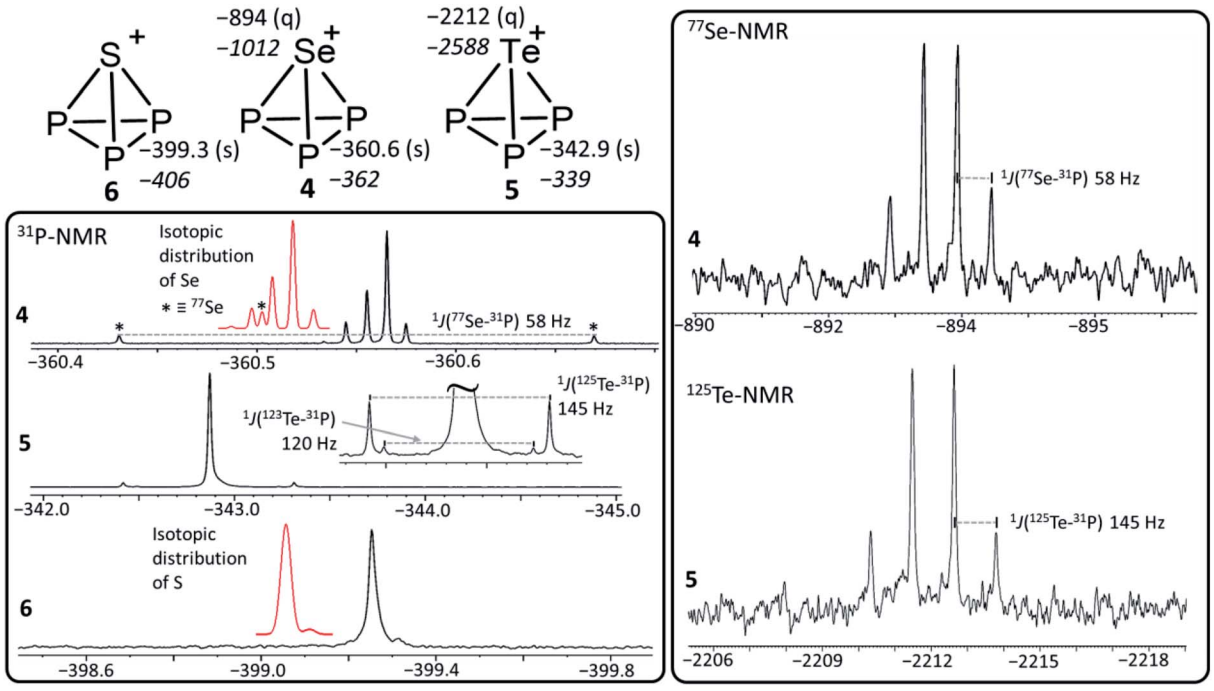

Fig. 1 Summary of the experimental and calculated (in *italics*) NMR data of **4**, **5** and **6** (top left) including a graphical representation of the structures of $[EP_3]^+$ (E = S, Se, Te). ^{77}Se (top right) and ^{125}Te (bottom right) spectra of **4** and **5** as well as the ^{31}P spectra of **4**, **5** and **6** (bottom left). The red traces in the ^{31}P-NMR box indicate the isotopic distributions of Se and S calculated with a standard mass spectrometry program. Of all noticeable S and Se isotopes, only ^{77}Se is NMR active (^{33}S has an abundancy of only 0.7%). Thus, only the NMR signal of $[^{77}Se^{31}P_3]^+$, labelled by an asterisk in the isotopic distribution, is visibly splitted to a doublet in the NMR trace of **4**. Apparently, the ^{31}P-chemical shift of $[EP_3]^+$ follows the weight of the isotopes for the lighter elements S and Se, with higher isotope weights leading to incrementally slightly higher field shifted ^{31}P-NMR resonances. However, for Te, where the relative weight differences between isotopomers are smallest among the three cations, the high-field shift in the ^{31}P-NMR is so small that the signals due to all Te-isotopes fall onto one visible line (with the exception of the two NMR active nuclei ^{123}Te and ^{125}Te that couple and give doublets).

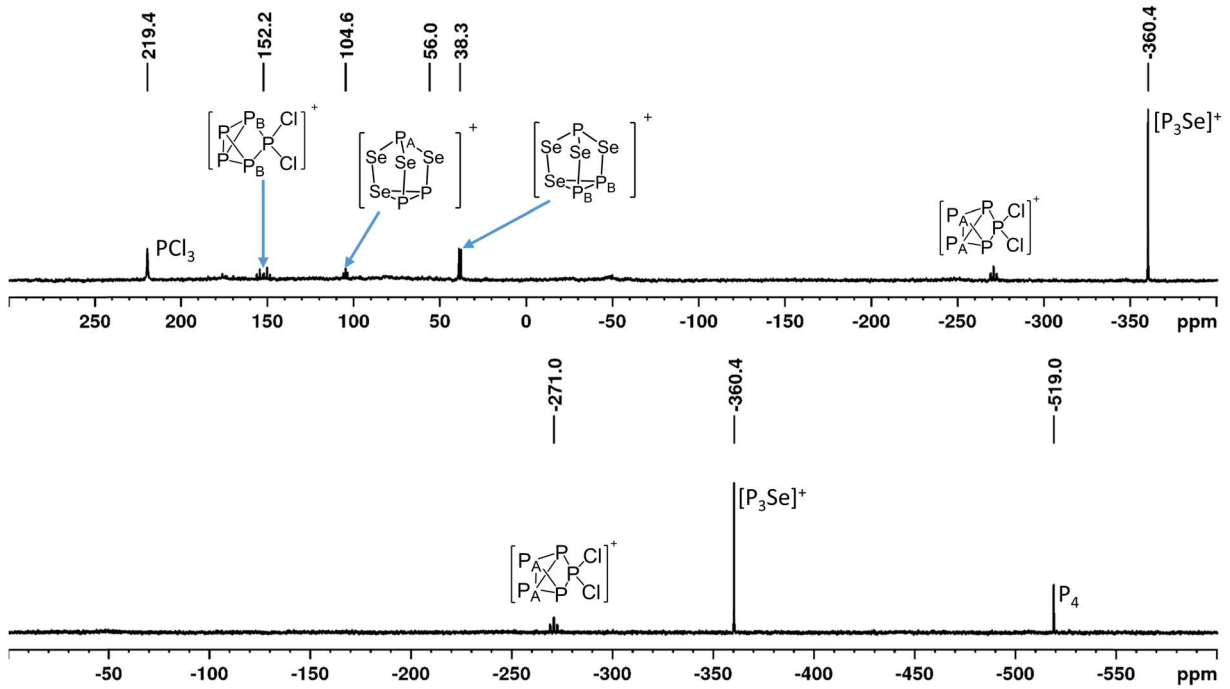

Fig. 2 Product ion mixture obtained from the larger scale reaction of **1a** with P_4 at −40 °C. Combined views of the measured range of the ^{31}P-NMR spectra (81.0 MHz, CD_2Cl_2, RT) from 300 to −400 ppm (top) and 0 to −600 ppm (bottom).

overlapping vibrational bands of the $[SeP_3]^+$, $[P_5Cl_2]^+$ and $[P_3Se_4]^+$ cations, as well as some Se_2Cl_2 showing its most intense band[33] at 361 cm^{-1} (ESI, Section 3.4.3.2†). An exact assignment of all vibrational bands is not possible due to the unavoidable occurrence of $[P_5Cl_2]^+$ having strong overlaps with the predicted bands of $[P_3Se]^+$. Electro-spray-MS spectra of solutions containing **4** showed the presence of the $[SeP_3]^+$ ($m/z = 172.83$) and the $[P_5Cl_2]^+$ ($m/z = 225.0$) cation (ESI, Section 3.4.3.2†).

On the occurrence of $[P_5Cl_2]^+$. The formation of **4**, **5** and **6** is necessarily accompanied by the formation of PCl_3 (eqn (3)). From NMR investigations it became clear that the $[EP_3]^+$ cations are unreactive towards PCl_3. On the other hand, the formation of $[P_5L_2]^+$ (L = organic residue or halide) cations is typically ascribed to the insertion of an intermediate carbene-like $[PL_2]^+$ into P_4.[1,5,27,34] However, this intermediate $[PCl_2]^+$ was never observed in the condensed phase, but assumed to be a complex $[(S)Ag–Cl–PCl_2]^+$ (S = solvent) delivering $[PCl_2]^+$ *in situ*.[35] To completely rule out the $[P_5Cl_2]^+$ presence as a byproduct ion resulting from the reaction of residual Ag^+ with PCl_3 and P_4, ion **4** was synthesized from a silver-free $SeCl_3[Al(OR^F)_4]$ prepared from $SeCl_4$ *via* the thallium salt[36] $Tl[Al(OR^F)_4]$ according to eqn (1). Yet, these experiments revealed a similar quantity of $[P_5Cl_2]^+$ as side product ion. Thus, the formation of $[P_5Cl_2]^+$ does not occur due to silver impurities of the starting material and may arise by reaction of P_4 with $[ECl_3]^+$ as in eqn (4).

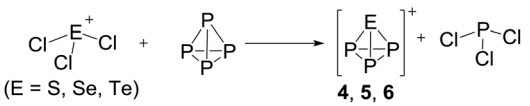

(3)

Table 1 Experimental and calculated (B3-LYP/DKH2/cc-PVQZ level, based on (RIJ)MP2/def2-QZVPP structures) $^{31}P/^{77}Se/^{125}Te$-NMR shifts, NICS values, bond lengths in the optimized structures and $^1J(P, E)$ coupling constants. The chemical shifts are given in ppm. Calculated data is given in *italics*

Compound	$\delta(^{31}P)^a$	NICS[b]	NICS/e[b]	d(P–E) [pm]	d(P–P) [pm]	$\delta(E)_{exp.}$[c]	$^1J(P, E)$
P_4	−520 *−520*	*−61.9*	*−3.10*	—	219.94(3)[37] *219.3*	—	—
AsP_3	−484 (ref. 2) *−484*	*−61.3*	*−3.07*	230.4(1)[37] *230.4*	219.5(3)[37] *219.4*	—	—
SbP_3	−462 (ref. 2) *−452*	*−58.6*	*−2.93*	*250.0*	*219.8*	—	—
$[SP_3]^+$	−399 *−406*	*−60.6*	*−3.03*	*214.8*	*220.2*	—	—
$[SeP_3]^+$	−361 *−362*	*−60.3*	*−3.02*	*228.1*	*220.5*	−894 *−1012*	$^1J(^{31}P, ^{77}Se) = 58$ Hz
$[TeP_3]^+$	−342 *−339*	*−59.4*	*−2.97*	*246.9*	*220.9*	−2212 *−2588*	$^1J(^{31}P, ^{125}Te) = 145$ Hz, $^1J(^{31}P, ^{123}Te) = 120$ Hz

[a] ^{31}P chemical shifts were referenced to the chemical shift of P_4 in CH_2Cl_2. [b] NICS values are calculated at the cage center. NICS/e denotes the NICS per valence electron. [c] ^{77}Se and ^{125}Te chemical shifts were referenced against the chemical shifts of $SePMe_3/TePMe_3$ more details on the referencing of the chemical shifts is given in the ESI in Section 4.2.

Table 2 *Ab initio* CCSD(T)/∞ζ reaction enthalpies and free reaction enthalpies for the formation of $[EP_3]^+$ (E = S, Se (parentheses), Te [brackets]) and the fluoride ion affinities (FIAs) of $[EP_3]^+$ and $[EX_3]^+$ (E = S, Se, Te; X = F, Cl, Br, I) cations [all given in kJ mol^{-1}]. Further details are given in the ESI in Tables S14 and S15

Reaction	E =	Δ_rH^{298} (g)	Δ_rG^{298} (g)	Δ_rG^{298} $(CH_2Cl_2)^b$	Δ_rG^{298} (*o*-dfb)^b	Δ_rG^{298} $(SO_2)^b$	Cation	FIA	E =
$P_4 + [EF_3]^+ \rightarrow [EP_3]^+ + PF_3$	S	−550	−554	−477	−475	−474	$[EF_3]^+$	909	S
	(Se)	(−560)	(−563)	(−468)	(−464)	(−463)		(941)	(Se)
	[Te]	[−407]	[−408]	[−319]	[−315]	[−314]		[962]	[Te]
$P_4 + [ECl_3]^+ \rightarrow [EP_3]^+ + PCl_3$	S	−339	−343	−324	−325	−325	$[ECl_3]^+$	775	S
	(Se)	(−291)	(−295)	(−269)	(−268)	(−268)		(803)	(Se)
	[Te]	[−167]	[−170]	[−143]	[−143]	[−142]		[844]	[Te]
$P_4 + [EBr_3]^+ \rightarrow [EP_3]^+ + PBr_3$	S	−263	−267	−271	−272	−273	$[EBr_3]^+$	735	S
	(Se)	(−206)	(−210)	(−209)	(−210)	(−210)		(762)	(Se)
	[Te]	[−97]	[−99]	[−96]	[−97]	[−97]		[805]	[Te]
$P_4 + [EI_3]^+ \rightarrow [EP_3]^+ + PI_3$	S	−165	−168	−184	−186	−187	$[EI_3]^{+a}$	675^a	S
	(Se)	(−115)	(−118)	(−127)	(−129)	(−129)		(704)	(Se)
	[Te]	[−29]	[−32]	[−39]	[−41]	[−41]		[753]	[Te]
$\frac{5}{4}P_4 + [ECl_3]^+ \rightarrow [P_5Cl_2]^+ + \frac{1}{2}E_2Cl_2$	S	−297	−267	−227	−225	−225	$[EP_3]^+$	828	S
	(Se)	(−256)	(−226)	(−182)	(−181)	(−180)	(F bound *via* P)	(819)	(Se)
	[Te]	[−152]	[−121]	[−84]	[−82]	[−82]		[798]	[Te]

^{a} Efforts to synthesize $[SI_3]^+$ previously yielded $[S_2I_4]^{2+}$ instead.[43] ^{b} The free reaction energies in solvents were calculated at the (RIJ)BP86/def2-TZVPP level using the COSMO model.

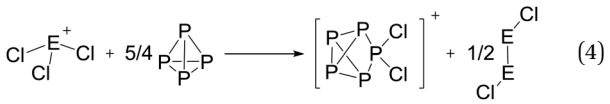

(4)

The reaction course according to eqn (4) is further supported by the observation of a yellow volatile material (Se_2Cl_2) present in the traps of the vacuum line after pumping on the mixtures as well as the Se_2Cl_2 Raman band observed in solid product mixtures at 361 cm^{-1} (ESI, Section 3.1†). Efforts to suppress this side reaction by slowly adding P_4 to the reaction at low temperatures showed no significant improvement towards a clean reaction (ESI, Table S7†).

Further side product ions. The known[20] $[P_3Se_4]^+$ additionally occurs as a side product ion. Performing the reaction at −40 °C lowers the amount of obtained $[P_3Se_4]^+$, but does not allow to completely get rid of this side product ion. Depending on the solvent, the higher chlorinated oxidized $[PCl_4]^+$ was also observed (ESI, Section 3.4.1†). An unknown side product/product ion including five chemically equivalent phosphorus atoms and three chemically equivalent tellurium atoms occurs during the synthesis of **5**. Analogously, in the synthesis of **6**, side-products of unknown origin occurred (ESI, Section 3.4.3†).

Quantum chemical calculations on $[EP_3]^+$

Since it proved impossible to crystallize any $[EP_3]^+$ salt, we turned to quantum chemical calculations, to shed some light on energetics, structure, properties and bonding.

Calculated structure and NMR-shifts

Molecular structures. The molecular structures of the title tetrahedra were calculated at the (RIJ)MP2/def2-QZVPP level, which gives very good agreement with experimental data for P_4 and PnP_3 (Pn = As, Sb). Apparently, the calculated $[EP_3]^+$ bond lengths d_{PP} are slightly elongated, if compared to the neutral tetrahedra and increase from S to Se to Te.

Calculated NMR-shifts. The calculated NMR-shifts of **4**, **5** and **6**, as well as that of the neutral molecules AsP_3 and SbP_3 for comparison, were obtained using a fully decontracted basis set with (RIJ)B3-LYP(DKH2)/cc-pVQZ single point calculations, using the (RIJ)MP2/def2-QZVPP structures. They were referenced against P_4 (Table 1). The calculated ^{31}P chemical shifts of all $[EP_3]^+$ ions deviate by less than 7 ppm from the experimental values. This is similar to the deviation of the calculated NMR shifts from the known AsP_3 and SbP_3 shifts (less than 10 ppm).[2] However, the calculated ^{77}Se and ^{125}Te chemical shifts show larger deviations from the experimental values. Yet, the trends in chemical shifts are well reproduced, as investigated on a larger test set of Se- and or Te-containing molecules spanning a range of 2300 ppm (Se) and even 5000 ppm (Te) (ESI, Section 4.2†). With such a broad range of chemical shifts, the choice of the reference compound is crucial, although the calculated absolute shielding tensors remain the same. Yet, no truly close relative to $[EP_3]^+$ is known experimentally to serve as a reference to tie to the calculated shift. The best compromise was to use $EPMe_3$ (E = Se, Te). We note, that the observed resonances of **4** and **5** underlie an extreme high-field shift to untypical regions for inorganic Se(IV) and Te(IV) compounds compared to their $[ECl_3]^+$ counterparts. This raises the question, whether the chalcogen atoms in the $[EP_3]^+$ cations can be formally rationalized as deriving from an E^{4+} cation being exposed to the ring current of a 6π Hückel-aromatic $[P_3]^{3-}$ ring or if the chalcogen atoms exhibit a lower formal oxidation state (see next section).

Bonding within $[EP_3]^+$. Since the $[EP_3]^+$ cations present a hitherto unknown class of cations in the condensed phase, an investigation of its bonding motifs is appropriate. With the unusually high-field shifted Se- and Te-NMR resonances at

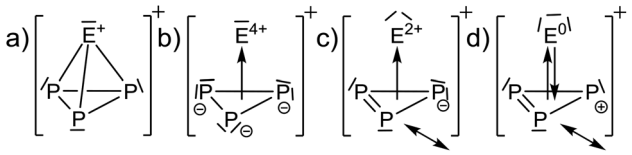

Scheme 2 Extreme, limiting sketches that might contribute to the $[EP_3]^+$ structures. (a) Formally electron precise structure, (b) cluster bonding as described by π-donation from a 6π Hückel-aromatic P_3^{3-} unit. (c) Similar, but π-donation from a 4π antiaromatic P_3^- and (d) synergistic π-donation from a 2π Hückel-aromatic P_3^+ unit to an E^0 and back bonding from p-type AOs of E^0 to π*-MOs of P_3^+.

−894 (Se) and −2212 (Te, Table 1), one could draw the following extreme, limiting sketches in Scheme 2a–d that might contribute to the $[EP_3]^+$ structures.

Thus, with the cluster-like description as in Scheme 2b and c, one would expect that the E atoms experience a large high-field shift due to the proximity to an aromatic ring current. Thus, it first needed to be investigated, if diamagnetic ring currents are present.

NICS values. Calculated nuclear independent chemical shift (NICS) values at the cage centers of the $[EP_3]^+$ cations suggest pronounced diamagnetic ring currents with a very slightly decreased order of magnitude, if compared with P_4 and AsP_3 (Table 1). This suggests a delocalized cluster-like bonding.

Population analyses and MO diagram. Calculated NBO, PABOON and AIM charges (Fig. 3) only agree that the positive charge on the E atom of the $[EP_3]^+$ cluster increases in going from S to Se and Te and that on P decreases in the same direction. The similarity of the calculated MO diagrams to the known[7] MO diagrams of P_4 and AsP_3 clearly shows that the $[EP_3]^+$ cations can be understood as clusters related to AsP_3 and P_4. This is in accordance with the generally at very high field observed NMR shifts as well as the NICS values in Table 1, and similar to the known tetrahedra P_4, AsP_3, Si_4^{4-} and Sn_4^{4-}.[2,14] However, closer inspection reveals some differences. First, due to the cationic nature, all orbital energies are lowered by 6 to 7 eV in comparison to the neutral tetrahedra. Second, the lowering of the symmetry from T_d to C_{3v} in AsP_3 splits the t_2-MOs of P_4 giving a pair of e and a_1 MOs. The sequence of orbital energies for this pair of e (higher *E*) and a_1 MOs (lower *E*) in AsP_3 matches those in $[EP_3]^+$ only for Se and Te. For the $[SP_3]^+$ system, these orbitals are reversed in energy and the a_1 MO is now higher in energy than the e MO (Fig. 3).

The HOMO LUMO gaps decrease in the order $[SP_3]^+$ (6.2 eV) > $[SeP_3]^+$ (5.9 eV) > $[TeP_3]^+$ (5.4 eV) and are comparable to P_4 and AsP_3 (6.4 eV and 6.0 eV with the same method). This speaks for a stable structure and bonding within $[EP_3]^+$. Closer inspection of the MOs in view of the descriptions in Scheme 2 would be in agreement with the suggestion that the back bonding component from p-type AOs of E^0 to π*-MOs of P_3^+ (Scheme 2d), which might be assigned to the e MO at −14.89 (S)/−14.24 (Se)/−13.37 (Te) eV in Fig. 3, is inferior for the heavier elements. Thus, apparently the sizes of the heavier p-type AOs do not fit similarly well as that of sulfur and the respective MO energies increase from S to Te.

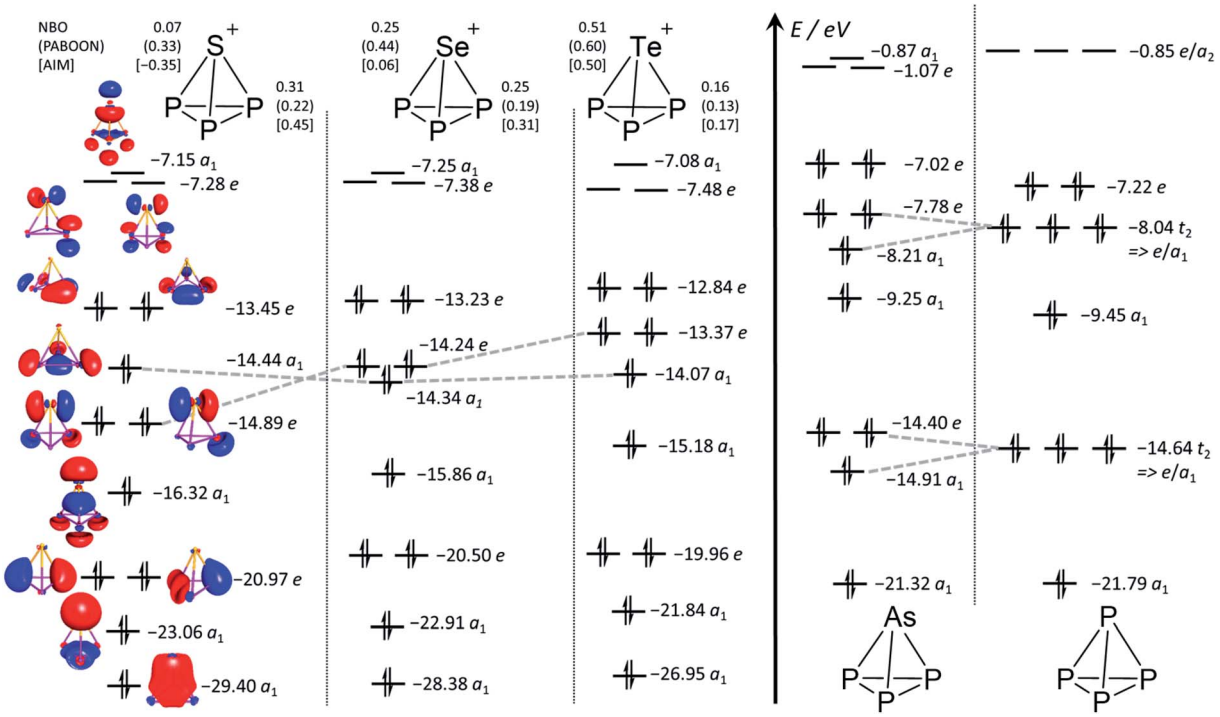

Fig. 3 Calculated MO Diagrams and NBO,[38] PABOON and AIM[39] charges of $[EP_3]^+$ ((RIJ)B3-LYP/def2-TZVPP). The corresponding MO diagrams of P_4 and AsP_3 were also generated and are in accordance with the previously published MO diagrams (*cf.* also ESI Section 4.1†).[7] The grey broken lines delineate the switch of the a_1 and e MO energies in going from E = S to Se and Te as well as the splitting of the t_2 MOs in P_4 upon symmetry lowering in AsP_3.

Further AIM analyses. Contour plots of the Laplacian of the electron density (Section 4.2, ESI†) show a similar situation for all $[EP_3]^+$ cations. They are closely related to the neutral molecules AsP_3 and P_4, with $[P_3S]^+$ being similar to P_4 and $[P_3Se]^+$ and $[P_3Te]^+$ being more similar to AsP_3. Exohedral lone pairs of the clusters are absent for any of the tetrahedra, which confirms the nature of the tetrahedra as delocalized clusters rather than electron precise molecules. The electron densities (ρ_{XCP}) residing at the critical points XCP (X = R (ring), C (cluster), B (bond)) of the $[EP_3]^+$ cations have similar values to P_4 and AsP_3 and are included with the ESI.† It is worth noting that the calculated increasing bond ellipticities for E = Se and Te would be in agreement with a description as in Scheme 2d and suggest a larger electronic separation of the 'E'- and 'P_3'-parts for the heavier elements and its interpretation as resulting from π-interactions.

Formation energetics of $[EP_3]^+$. To provide reliable values, the thermodynamics of the product ion mixture formation was assessed using the gold standard of quantum chemistry, the coupled cluster level of theory with single, double and a numerical evaluation of the triples excitation extrapolated to the complete basis set limit (CCSD(T)/$\infty\zeta$, see ESI†), an approach we have shown to be accurate within about 5 kJ mol^{-1}.[29,40] Reaction enthalpies and Gibbs energies with and without solvation calculated towards the formation of $[EP_3]^+$ from $[EX_3]^+$ (X = F–I) and P_4 are collected in Table 2. They are in agreement with the observed formation of ions **4** to **6** from $[ECl_3]^+$, but also agree with the competing formation of the chlorinated side product ion $[P_5Cl_2]^+$ (eqn (4) and Table 2). Thus, for E = Se, $[P_5Cl_2]^+$ formation is exergonic ($\Delta_rG^\circ = -180$ to -182 kJ mol^{-1} in solution) as is the formation of $[EP_3]^+$ ($\Delta_rG^\circ = -268$ to -269 kJ mol^{-1} in solution). Apparently, the competing formation of $[P_5Cl_2]^+$ has kinetic reasons. With all our tested conditions, any clear discrimination between both routes was impossible. This suggests that the activation barriers to reach the two product ions $[P_5Cl_2]^+$ and $[EP_3]^+$ starting from ECl_3^+ and P_4 have similar height and cannot be selectively favored by all the tested measures. This raised the question, as to whether it would be favorable to change the chloride ligands in $[ECl_3]^+$ for other halides to improve selectivity. Inspection of Table 2 shows that the driving force for $[EP_3]^+$ formation from P_4 and $[EX_3]^+$ lowers in the sequence F > Cl > Br > I but also S > Se > Te. Only the fluoro-chalcogenonium salts $EF_3[A]$ would provide a considerably higher impetus to yield $[EP_3]^+$, presumably due to formation of the very stable PF_3 gas. However, the $[EF_3]^+$ ions are extreme Lewis acids, as shown by their calculated very high fluoride ion affinities (FIAs, Table 2). Their Lewis acidity increases from S (909 kJ mol^{-1}) to Te (FIA 961 kJ mol^{-1}). These FIA values are close to that of the extremely Lewis acidic small silylium ion $[SiMe_3]^+$ (+958 kJ mol^{-1}).[41] The latter, *in situ* generated from Me_3SiCl and $Ag[Al(OR^F)_4]$, reacts with the $[Al(OR^F)_4]^-$ anion under fluoride abstraction to give the adduct $Me_3Si–F–Al(OR^F)_3$ and the epoxide C_4F_8O.[26,42] Thus, at least $[SeF_3]^+$ and $[TeF_3]^+$ should be, according to our experience, unstable with the aluminates used as counterions in this study. By contrast and in agreement with the experiment, the FIA values of the $[EP_3]^+$ ions of 798 to 828 kJ mol^{-1} are in a range that is typically tolerated by the $[Al(OR^F)_4]^-$ anion.

$[SF_3]^+$ with a FIA of 915 kJ mol^{-1}, similar to the one of $[CCl_3]^+$ (904 kJ mol^{-1})[44] that is stable as $[Al(OR^F)_4]^-$ salt and in solution at temperatures of −20 °C,[45] might be accessible with the aluminate counterions. Therefore, we have tried to prepare the salt $SF_3[Al(OR^F)_4]$, but all efforts failed and no $[EF_3]^+$ salts could be tested. However, this might be a reaction path that could be pursued in future; given the use of a suitable WCA tolerant towards extremely Lewis acidic cations – for example a halogenated carborane anion. As to whether the strongly exergonic Gibbs energy for the formation of the $[EP_3]^+$ cations from $[EF_3]^+$ salts and P_4 would guarantee a selective reaction, remains to be tested. However, we do not expect that fluorometallates $[MF_6]^-$ (M = P, As, Sb), with considerably lower FIA values of MF_5 (389 to 495 kJ mol^{-1}) than $Al(OR^F)_3$ (543 kJ mol^{-1}),[41] would stabilize salts of $[EP_3]^+$, but rather form fluoro-phosphorus compounds and MF_5.

Conclusion

Investigations on the existence of tetrahedral $[EP_3]^+$ (E = S, Se, Te) in condensed phases required the here reported synthesis and characterization of well-soluble salts $ECl_3[WCA]$. We note, that these cations are very strong Lewis acids with FIA values of 775 (S); 803 (Se) and 844 (Te) kJ mol^{-1} that could be relevant in view of the renewed interest[46] in strong[47] (also cationic[48]) Lewis acids.[49] They should be compared to classical phosphenium ions $[PR_2]^+$ with FIA values of 721 (R = NMe_2), 789 (R = Mes) and 828 (R = Ph).[50] The easily and in high yield accessible salts $ECl_3[WCA]$ were tested for their reaction with the known P_3^{3-} precursor $Na[Nb(P_3)(ODipp)_3]$, related to the synthesis of AsP_3 from $AsCl_3$. Only a clean generation of P_4 occurred. This is due to the strongly chlorinating nature of the $[ECl_3]^+$ cations that immediately reacted with the niobate to give PCl_3. Subsequently, the PCl_3 was transformed by the P_3-niobate to P_4. Contrary, the reaction of the salts $ECl_3[WCA]$ with P_4, led to reaction mixtures containing mainly the $[EP_3]^+$ cations, PCl_3 and $[P_5Cl_2]^+$ as well as other byproducts/byproduct ions. Even under optimized reaction conditions, the clean formation of $[EP_3]^+$ and PCl_3 from $[ECl_3]^+$ and P_4 is rivaled by side reactions. High level quantum chemical calculations show that the formation of $[EP_3]^+$ and of $[P_5Cl_2]^+$ are both strongly exergonic and independent of the solvent choice. Apparently, the similar activation energies of the reactions prevent the separation of both pathways by all tested reaction conditions. Experimental ^{31}P-, ^{77}Se- and ^{125}Te-NMR spectra as well as calculations of the chemical shifts prove the presence of the first cationic tetrahedra in the condensed phase. The selenium analogue $[SeP_3]^+$ was also unambiguously detected by ESI-MS of the obtained samples, while IR- and Raman spectra show the expected mixtures of cations in agreement with the optimized NMR conditions. The $[EP_3]^+$ ions are the first tetrahedral cations stabilized in the condensed phase, contrasted by the many anionic and the long known neutral tetrahedra. These cationic tetrahedra are also the first clear evidence for binary P–S and P–Te cations in the condensed phase, with the 2015 published

$[P_3Se_4]^+$ being the first phosphorus chalcogen cation at all. Theoretical investigations show, that the $[EP_3]^+$ tetrahedra can be understood as clusters similar to P_4 and AsP_3 as indicated by their MO diagrams, AIM analyses and calculated NICS values. The unusually high-field shifted ^{77}Se- and ^{125}Te-NMR shifts may arise from a synergistic π-interaction between formal E^0 and P_3^+ fragments.

Conflicts of interest

There are no conflicts to declare.

Acknowledgements

This work was supported by the Albert-Ludwigs-Universität Freiburg and by the DFG in the *Normalverfahren*. We would like to thank Fadime Bitgül and Dr Arthur Martens for the measurement of NMR spectra and Dr Daniel Himmel for valuable discussions concerning the DFT and *ab initio* calculations.

References

1 J. J. Weigand, M. Holthausen and R. Fröhlich, *Angew. Chem., Int. Ed.*, 2009, **48**, 295.
2 B. M. Cossairt, M.-C. Diawara and C. C. Cummins, *Science*, 2009, **323**, 602.
3 (*a*) L. C. Forfar, T. J. Clark, M. Green, S. M. Mansell, C. A. Russell, R. A. Sanguramath and J. M. Slattery, *Chem. Commun.*, 2012, **48**, 1970; (*b*) S. Heinl, E. V. Peresypkina, A. Y. Timoshkin, P. Mastrorilli, V. Gallo and M. Scheer, *Angew. Chem., Int. Ed.*, 2013, **52**, 10887; (*c*) F. Hennersdorf, J. Frötschel and J. J. Weigand, *J. Am. Chem. Soc.*, 2017, **139**, 14592; (*d*) M. H. Holthausen, S. K. Surmiak, P. Jerabek, G. Frenking and J. J. Weigand, *Angew. Chem., Int. Ed.*, 2013, **52**, 11078; (*e*) M. Ichinohe, M. Toyoshima, R. Kinjo and A. Sekiguchi, *J. Am. Chem. Soc.*, 2003, **125**, 13328; (*f*) I. Krossing and L. van Wüllen, *Chem.–Eur. J.*, 2002, **8**, 700; (*g*) P. Mal, B. Breiner, K. Rissanen and J. R. Nitschke, *Science*, 2009, **324**, 1697; (*h*) T. Mennekes, P. Paetzold, R. Boese and D. Bläser, *Angew. Chem., Int. Ed.*, 1991, **30**, 173; (*i*) F. Meyer-Wegner, S. Scholz, I. Sänger, F. Schödel, M. Bolte, M. Wagner and H.-W. Lerner, *Organometallics*, 2009, **28**, 6835; (*j*) S. Mitzinger, L. Broeckaert, W. Massa, F. Weigend and S. Dehnen, *Nat. Commun.*, 2016, **7**, 10480; (*k*) C. Schwarzmaier, A. Schindler, C. Heindl, S. Scheuermayer, E. V. Peresypkina, A. V. Virovets, M. Neumeier, R. Gschwind and M. Scheer, *Angew. Chem., Int. Ed.*, 2013, **52**, 10896; (*l*) F. Spitzer, M. Sierka, M. Latronico, P. Mastrorilli, A. V. Virovets and M. Scheer, *Angew. Chem., Int. Ed.*, 2015, **54**, 4392; (*m*) M. Waibel and T. F. Fässler, *Z. Naturforsch., B: J. Chem. Sci.*, 2013, **68**, 732; (*n*) J. E. Borger, A. W. Ehlers, M. Lutz, J. C. Slootweg and K. Lammertsma, *Angew. Chem., Int. Ed.*, 2014, **53**, 12836; (*o*) I. de los Rios, J.-R. Hamon, P. Hamon, C. Lapinte, L. Toupet, A. Romerosa and M. Peruzzini, *Angew. Chem., Int. Ed.*, 2001, **40**, 3910.
4 C. Schwarzmaier, M. Sierka and M. Scheer, *Angew. Chem., Int. Ed.*, 2013, **52**, 858.
5 M. H. Holthausen, K.-O. Feldmann, S. Schulz, A. Hepp and J. J. Weigand, *Inorg. Chem.*, 2012, **51**, 3374.
6 (*a*) J. P. Zheng, J. Waluk, J. Spanget-Larsen, D. M. Blake and J. G. Radziszewski, *Chem. Phys. Lett.*, 2000, **328**, 227; (*b*) P. Jerabek and G. Frenking, *Theor. Chem. Acc.*, 2014, **133**, 1447; (*c*) E. E. Rennie and P. M. Mayer, *J. Chem. Phys.*, 2004, **120**, 10561.
7 B. M. Cossairt and C. C. Cummins, *J. Am. Chem. Soc.*, 2009, **131**, 15501.
8 A. E. Seitz, F. Hippauf, W. Kremer, S. Kaskel and M. Scheer, *Nat. Commun.*, 2018, **9**, 361.
9 T. A. Engesser, W. J. Transue, P. Weis, C. C. Cummins and I. Krossing, *Eur. J. Inorg. Chem.*, 2019, **2019**, 2607.
10 A. Wiesner, S. Steinhauer, H. Beckers, C. Müller and S. Riedel, *Chem. Sci.*, 2018, **9**, 7169.
11 (*a*) M. Baitinger, Y. Grin, R. Kniep and H. G. von Schnering, *Z. Kristallogr.*, 1999, 214; (*b*) M. Baitinger, K. Peters, M. Somer, W. Carrillo-Cabrera, Y. Grin, R. Kniep and H. G. von Schnering, *Z. Kristallogr.*, 1999, 214; (*c*) A. Betz, H. Schäfer, A. Weiss and R. Wulf, *Z. Naturforsch., B: Anorg. Chem., Org. Chem., Biochem., Biophys., Biol.*, 1968, **23**, 878; (*d*) S. Bobev and S. C. Sevov, *Polyhedron*, 2002, **21**, 641; (*e*) E. Busmann, *Z. Anorg. Allg. Chem.*, 1961, **313**, 90; (*f*) J. Curda, W. Carrillo-Cabrera, A. Schmeding, K. Peters, M. Somer and H. G. von Schnering, *Z. Anorg. Allg. Chem.*, 1997, **623**, 929; (*g*) I. F. Hewaidy, E. Busmann and W. Klemm, *Z. Anorg. Allg. Chem.*, 1964, **328**, 283; (*h*) C. Hoch and C. Röhr, *Z. Anorg. Allg. Chem.*, 2002, **628**, 1541; (*i*) C. Hoch, M. Wendorff and C. Röhr, *Z. Anorg. Allg. Chem.*, 2003, **629**, 2391; (*j*) C. Hoch, M. Wendorff and C. Röhr, *J. Alloys Compd.*, 2003, **361**, 206; (*k*) K. H. Janzon, H. Schäfer and A. Weiss, *Z. Anorg. Allg. Chem.*, 1970, **372**, 87; (*l*) J. Llanos, R. Nesper and H. G. von Schnering, *Angew. Chem.*, 1983, **95**, 1026; (*m*) R. E. Marsh and D. P. Shoemaker, *Acta Crystallogr.*, 1953, **6**, 197; (*n*) V. Quéneau, E. Todorov and S. C. Sevov, *J. Am. Chem. Soc.*, 1998, **120**, 3263; (*o*) C. Röhr, *Z. Naturforsch., B: J. Chem. Sci.*, 1995, **50**, 802; (*p*) R. Schäfer and W. Klemm, *Z. Anorg. Allg. Chem.*, 1961, **312**, 214; (*q*) H. G. von Schnering, M. Baitinger, U. Bolle, W. Carrillo-Cabrera, J. Curda, Y. Grin, F. Heinemann, J. Llanos, K. Peters, A. Schmeding and M. Somer, *Z. Anorg. Allg. Chem.*, 1997, **623**, 1037; (*r*) H. G. von Schnering, M. Schwarz and R. Nesper, *Angew. Chem., Int. Ed.*, 1986, **25**, 566; (*s*) J. Witte, H. G. Schnering and W. Klemm, *Z. Anorg. Allg. Chem.*, 1964, **327**, 260; (*t*) G. Cordier and W. Blase, *Z. Kristallogr.*, 1991, **196**, 207.
12 (*a*) R. Ababei, J. Heine, M. Hołyńska, G. Thiele, B. Weinert, X. Xie, F. Weigend and S. Dehnen, *Chem. Commun.*, 2012, **48**, 11295; (*b*) S. C. Critchlow and J. D. Corbett, *Inorg. Chem.*, 1982, **21**, 3286; (*c*) S. C. Critchlow and J. D. Corbett, *Inorg. Chem.*, 1985, **24**, 979; (*d*) F. Lips, M. Raupach, W. Massa and S. Dehnen, *Z. Anorg. Allg. Chem.*, 2011, **637**, 859; (*e*) F. Lips, I. Schellenberg, R. Pöttgen and S. Dehnen, *Chem.–Eur. J.*, 2009, **15**, 12968; (*f*) S. Mitzinger, J. Bandemehr, K. Reiter, J. Scott McIndoe, X. Xie,

F. Weigend, J. F. Corrigan and S. Dehnen, *Chem. Commun.*, 2018, **54**, 1421; (*g*) L. Xu and S. C. Sevov, *Inorg. Chem.*, 2000, **39**, 5383; (*h*) U. Friedrich, M. Neumeier, C. Koch and N. Korber, *Chem. Commun.*, 2012, **48**, 10544.

13 (*a*) C. B. Benda, T. Henneberger, W. Klein and T. F. Fässler, *Z. Anorg. Allg. Chem.*, 2017, **643**, 146; (*b*) F. Hastreiter, C. Lorenz, J. Hioe, S. Gärtner, N. Lokesh, N. Korber and R. M. Gschwind, *Angew. Chem., Int. Ed.*, 2019, 3133–3137; (*c*) C. Lorenz, S. Gärtner and N. Korber, *Z. Anorg. Allg. Chem.*, 2017, **643**, 141.

14 M. Neumeier, F. Fendt, S. Gärtner, C. Koch, T. Gärtner, N. Korber and R. M. Gschwind, *Angew. Chem., Int. Ed.*, 2013, **52**, 4483.

15 (*a*) G. J. Penney and G. M. Sheldrick, *J. Chem. Soc. A*, 1971, 243; (*b*) L. Operti, G. A. Vaglio, M. Peruzzini and P. Stoppioni, *Inorg. Chim. Acta*, 1985, **96**, 43.

16 D. A. Northrop, *Mater. Res. Bull.*, 1972, **7**, 147.

17 (*a*) M. Di Vaira, F. Mani, S. Moneti, M. Peruzzini, L. Sacconi and P. Stoppioni, *Inorg. Chem.*, 1985, **24**, 2230; (*b*) M. Di Vaira, M. Peruzzini and P. Stoppioni, *J. Chem. Soc., Chem. Commun.*, 1982, 894; (*c*) M. Di Vaira, M. Peruzzini and P. Stoppioni, *Polyhedron*, 1986, **5**, 945.

18 (*a*) M. F. Groh, A. Wolff, M. A. Grasser and M. Ruck, *Int. J. Mol. Sci.*, 2016, 17; (*b*) T. Chivers and I. Manners, *Inorganic rings and polymers of the p-block elements. From fundamentals to applications*, Royal Society of Chemistry, Cambridge, 2009; (*c*) J. Beck, S. Schlüter and N. Zotov, *Z. Anorg. Allg. Chem.*, 2005, **631**, 2450; (*d*) A. Eich, S. Schlüter, G. Schnakenburg and J. Beck, *Z. Anorg. Allg. Chem.*, 2013, **639**, 375; (*e*) J. Beck, S. Schlüter and N. Zotov, *Z. Anorg. Allg. Chem.*, 2004, **630**, 2512; (*f*) J. Beck, M. Dolg and S. Schlüter, *Angew. Chem., Int. Ed.*, 2001, **40**, 2287.

19 B. H. Christian, R. J. Gillespie and J. F. Sawyer, *Inorg. Chem.*, 1981, **20**, 3410.

20 K.-O. Feldmann, T. Wiegand, J. Ren, H. Eckert, J. Breternitz, M. F. Groh, U. Müller, M. Ruck, B. Maryasin, C. Ochsenfeld, O. Schön, K. Karaghiosoff and J. J. Weigand, *Chem.–Eur. J.*, 2015, **21**, 9697.

21 M. Donath, F. Hennersdorf and J. J. Weigand, *Chem. Soc. Rev.*, 2016, **45**, 1145.

22 T. M. Klapötke and C. M. Riencker, *Z. Anorg. Allg. Chem.*, 1994, **620**, 2104.

23 A structural characterization was not possible due to its insolubility in SO_2 and $CFCl_3$. A monomeric $[SeP]^+$ was disproven by vibrational spectra. Dissolution in HMPT, DMF, DMSO or MeOH led to spontaneous combustion and mechanical stress led towards explosion. Using other $[SeCl_3]^+$ salts such as $SeCl_3[SbCl_6]$ or $SeCl_3[AsF_6]$ failed due to the high affinity of phosphorus to fluorine or led to an even more sensitive material. Using solvents other than liquid PH_3 failed due to the insolubility of $SeCl_3[AlCl_4]$ in common organic solvents or the tendency to sidereactions due to the oxophilic nature of phosphorus in inorganic solvents such as SO_2.

24 T. A. Engesser, M. R. Lichtenthaler, M. Schleep and I. Krossing, *Chem. Soc. Rev.*, 2016, **45**, 789.

25 T. A. Engesser, P. Hrobárik, N. Trapp, P. Eiden, H. Scherer, M. Kaupp and I. Krossing, *ChemPlusChem*, 2012, **77**, 643.

26 A. Martens, P. Weis, M. C. Krummer, M. Kreuzer, A. Meierhöfer, S. C. Meier, J. Bohnenberger, H. Scherer, I. Riddlestone and I. Krossing, *Chem. Sci.*, 2018, **45**, 789.

27 A. Bihlmeier, M. Gonsior, I. Raabe, N. Trapp and I. Krossing, *Chem.–Eur. J.*, 2004, **10**, 5041.

28 (*a*) I. Krossing and I. Raabe, *Chem.–Eur. J.*, 2004, **10**, 5017; (*b*) A. Martens, M. Kreuzer, A. Ripp, M. Schneider, D. Himmel, H. Scherer and I. Krossing, *Chem. Sci.*, 2019, **10**, 2821.

29 J. Bohnenberger, W. Feuerstein, D. Himmel, M. Daub, F. Breher and I. Krossing, *Nat. Commun.*, 2019, **10**, 624.

30 $Tl[Al(OR^F)_4]$ forms no complex with P_4 which is beneficial for the removal of residual P_4 (see ESI Section 3.5†).

31 P. Weis, H. Scherer and I. Krossing, *Z. Anorg. Allg. Chem.*, 2019, **645**, 64.

32 The integral ratios are given in the ESI in Tables S7, S9 and S10.†

33 S. G. Frankiss, *J. Mol. Struct.*, 1968, **2**, 271.

34 (*a*) M. H. Holthausen and J. J. Weigand, *Dalton Trans.*, 2016, **45**, 1953; (*b*) M. H. Holthausen, A. Hepp and J. J. Weigand, *Chem.–Eur. J.*, 2013, **19**, 9895; (*c*) M. H. Holthausen, C. Richter, A. Hepp and J. J. Weigand, *Chem. Commun.*, 2010, **46**, 6921; (*d*) M. H. Holthausen, C. Sala and J. J. Weigand, *Eur. J. Inorg. Chem.*, 2016, **2016**, 667; (*e*) M. H. Holthausen and J. J. Weigand, *J. Am. Chem. Soc.*, 2009, **131**, 14210; (*f*) M. H. Holthausen and J. J. Weigand, *Z. Anorg. Allg. Chem.*, 2012, **638**, 1103; (*g*) I. Krossing and I. Raabe, *Angew. Chem., Int. Ed.*, 2001, **40**, 4406.

35 (*a*) M. Gonsior, I. Krossing and E. Matern, *Chem.–Eur. J.*, 2006, **12**, 1703; (*b*) N. Burford, C. A. Dyker and A. Decken, *Angew. Chem., Int. Ed.*, 2005, **44**, 2364; (*c*) N. Burford, P. J. Ragogna, R. McDonald and M. J. Ferguson, *J. Am. Chem. Soc.*, 2003, **125**, 14404.

36 Reactions of $Tl[Al(OR^F)_4]$ with PCl_3 have shown that no halide abstraction occurs with Tl^+ contrary to Ag^+ (see ESI Section 3.5†).

37 B. M. Cossairt, C. C. Cummins, A. R. Head, D. L. Lichtenberger, R. J. F. Berger, S. A. Hayes, N. W. Mitzel and G. Wu, *J. Am. Chem. Soc.*, 2010, **132**, 8459.

38 A. E. Reed, R. B. Weinstock and F. Weinhold, *J. Chem. Phys.*, 1985, **83**, 735.

39 R. F. W. Bader, *Acc. Chem. Res.*, 1985, **18**, 9.

40 (*a*) S. C. Meier, A. Holz, A. Schmidt, D. Kratzert, D. Himmel and I. Krossing, *Chem.–Eur. J.*, 2017, **23**, 14658; (*b*) M. M. Schwab, D. Himmel, S. Kacprzak, Z. Yassine, D. Kratzert, C. Felbek, S. Weber and I. Krossing, *Eur. J. Inorg. Chem.*, 2019, **2019**, 3309; (*c*) S. C. Meier, A. Holz, J. Kulenkampff, A. Schmidt, D. Kratzert, D. Himmel, D. Schmitz, E.-W. Scheidt, W. Scherer, C. Bülow, M. Timm, R. Lindblad, S. T. Akin, V. Zamudio-Bayer, B. von Issendorff, M. A. Duncan, J. T. Lau and I. Krossing, *Angew. Chem., Int. Ed. Engl.*, 2018, **57**, 9310.

41 H. Böhrer, N. Trapp, D. Himmel, M. Schleep and I. Krossing, *Dalton Trans.*, 2015, **44**, 7489.

42 M. Rohde, L. O. Müller, D. Himmel, H. Scherer and I. Krossing, *Chemistry*, 2014, **20**, 1218.

43 S. Brownridge, T. S. Cameron, H. Du, C. Knapp, R. Koppe, J. Passmore, J. M. Rautiainen and H. Schnöckel, *Inorg. Chem.*, 2005, **44**, 1660.
44 I. Krossing, A. Bihlmeier, I. Raabe and N. Trapp, *Angew. Chem., Int. Ed.*, 2003, **42**, 1531.
45 A. J. Lehner, N. Trapp, H. Scherer and I. Krossing, *Dalton Trans.*, 2011, **40**, 1448.
46 L. Greb, *Chem.–Eur. J.*, 2018, **24**, 17881.
47 J. F. Kögel, D. A. Sorokin, A. Khvorost, M. Scott, K. Harms, D. Himmel, I. Krossing and J. Sundermeyer, *Chem. Sci.*, 2018, **9**, 245.
48 H. Zhao and F. P. Gabbaï, *Nat. Chem.*, 2010, **2**, 984.
49 A. R. Jupp, T. C. Johnstone and D. W. Stephan, *Inorg. Chem.*, 2018, **57**, 14764.
50 J. M. Slattery and S. Hussein, *Dalton Trans.*, 2012, **41**, 1808.